

THE VARIATIONAL APPROACH TO RATE-INDEPENDENT PROCESSES

Gianpietro DEL PIERO¹

Communicated to:

9-ème Colloque franco-roumain de math. appl., 28 août-2 sept. 2008, Braşov, Romania

Abstract

Two one-dimensional variational models involving a cohesive energy are discussed. In the first model the cohesive energy is recoverable, and in the second it is dissipative. The first model captures the response of several classes of inelastic materials at loading, but fails to properly describe the response at unloading. This goal is achieved by the dissipative model.

2000 *Mathematics Subject Classification*: 74A45, 74A20, 74R99.

1 Introduction

The variational approach is frequently used for the mathematical characterization of material behavior. In it, the response of a material is obtained from the minimization of a functional which, in addition to the elastic strain energy, involves an energetic term due to inelastic phenomena such as fracture [2, 10], plasticity [3], or damage [9]. In particular, this second term may be the *cohesive energy* associated with jump discontinuities in the displacement field, in accordance with an idea of G.I. Barenblatt [1] which found large application in fracture mechanics. At present, due to the technical difficulties met in the multi-dimensional case, only the one-dimensional cohesive model has been satisfactorily developed. Only recently, some results of multi-dimensional analyses began to appear.

The present communication is based on the paper [7] by L. Truskinovsky and myself. In it two different models are discussed, in which the cohesive energy is assumed to be totally recoverable and totally dissipative, respectively. Depending on the analytical shape chosen for the cohesive energy, the *elastic* model reproduces the loading curves of different classes of materials. In addition, the *inelastic* models provides an accurate description of the behavior at unloading.

¹Università di Ferrara, Ferrara, Italy.

2 Materials with elastic cohesive energy

Consider a one-dimensional bar of length l which, due to axial displacements imposed at the two ends, undergoes a (possibly discontinuous) axial displacement u . The energy of the bar is

$$E(u) = \int_0^l w(u'(x)) dx + \sum_{x \in S(u)} \theta([u](x)), \quad (1)$$

where w is the strain energy density and θ is the cohesive energy. The first is a function of the bulk deformation u' and the second is a function of the jumps $[u]$ of u at the jump points x , which form the jump set $S(u)$. It is assumed that w is strictly convex, with $w(0) = w'(0) = 0$, and grows to infinity at extreme deformations in tension and in compression:

$$w(+\infty) = w(-1) = +\infty. \quad (2)$$

It is also assumed that θ is lower semicontinuous, with $\theta(0) = 0$, $\theta([u]) = +\infty$ for all $[u] < 0$, θ differentiable with $\theta'([u]) \geq 0$ in $(0, +\infty)$, and that the limits

$$\theta(0+) \doteq \lim_{[u] \rightarrow 0+} \theta([u]), \quad \theta'(0+) \doteq \lim_{[u] \rightarrow 0+} \frac{\theta([u])}{[u]}, \quad (3)$$

exist. The displacements at the ends are $u(0) = 0$, $u(l) = \beta l$, where βl is the prescribed total elongation of the bar. It determines the boundary condition

$$\int_0^l u'(x) dx + \sum_{S(u)} [u](x) = \beta l. \quad (4)$$

An *equilibrium configuration* is a displacement field u at which the first variation of E is non-negative

$$\lim_{\epsilon \rightarrow 0+} \frac{1}{\epsilon} (E(u + \epsilon \eta) - E(u)) \geq 0, \quad (5)$$

for all perturbations η which leave unchanged the total length of the bar. Notice that this is a necessary condition for a minimum at u , and that the inequality sign is appropriate because, due to the assumptions made on w and θ , the functional is non-smooth. It is proved in [7] that this condition is satisfied if and only if

- (i) the bulk deformation u' is the same at all x in $(0, l) \setminus S(u)$,
- (ii) the axial force at each jump point is equal to the axial force at the bulk points

$$\theta'([u](x)) = w'(u') \quad \forall x \in S(u), \quad (6)$$

- (iii) the axial force does not exceed the value $\theta'(0+)$.

Thus, in a bar at equilibrium the axial force has a constant value σ , and

$$\sigma \doteq w'(u') \leq \theta'(0+). \quad (7)$$

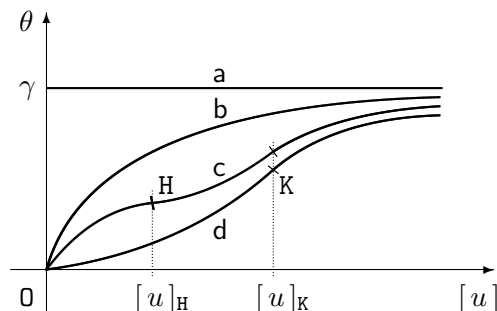


Figure 1: Some types of cohesive energy: (a) Griffith, (b) Barenblatt, (c) bi-modal, (d) convex-concave.

An equilibrium configuration is *metastable* if it is a local minimizer for E relative to the norm of the *total variation*

$$\|u\| \doteq \int_0^l |u'(x)| dx + \sum_{x \in S(u)} |[u](x)|. \quad (8)$$

It is proved in [7] that there are only two types of metastable configurations:

- (i) those for which $\theta''([u](x)) \geq 0$ for all x in $S(u)$,
- (ii) those with $\theta''([u](x)) > 0$ for all x in $S(u)$ except one, and with

$$\frac{l}{w''(u')} + \sum_{x \in S(u)} \frac{1}{\theta''([u](x))} \leq 0. \quad (9)$$

An *equilibrium process* is a one-parameter family $t \mapsto u_t$ of equilibrium configurations, continuous with respect to the norm (8). For a given equilibrium process, the relation (7)₁ determines the value σ_t of the axial force at t , and the boundary condition (4) determines the corresponding value β_t of the total elongation. The force-elongation relation

$$\sigma = \tilde{\sigma}(\beta) \quad (10)$$

determines the *force-elongation response curve* for the given process. The shape of this curve strongly depends on the analytical expression of the cohesive energy θ . Four possible choices are shown in Fig. 1. Let us briefly discuss the corresponding response curves.

1. In the case of Griffith's energy [11], θ is zero at $[u] = 0$ and takes a constant value γ at all positive $[u]$. Then, by (6, 7), $\sigma = 0$ at all $[u] > 0$, that is, the axial force is zero in every fractured equilibrium configuration. Moreover, by the assumptions made on w , the bulk deformation u' is zero as well, so that the total elongation βl is entirely due to the jumps $[u]$. There are, therefore, only two types of response curves:

- (i) $\sigma = w'(\beta)$ for unfractured configurations,
- (ii) $\sigma = 0$ for fractured configurations.

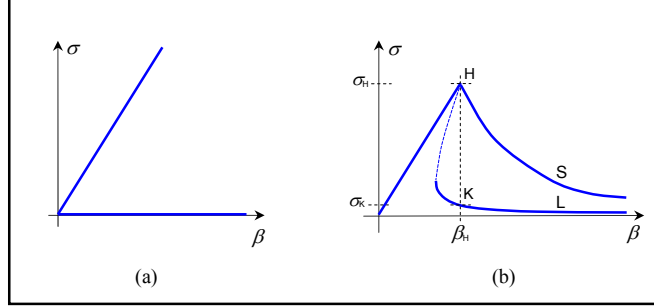


Figure 2: The response curves for the Griffith (a) and for the Barenblatt (b) cohesive energies.

They are shown in Fig. 2a.

2. The cohesive energy of Barenblatt [1] can be viewed as a regularization of the discontinuity at $[u] = 0$ exhibited by Griffith's energy. The function θ is assumed to be concave, $\theta''([u]) \leq 0$. Then, by the metastability condition, there can be at most one jump point in a metastable configuration. There are again only two types of response curves: the curve $\sigma = w'(\beta)$ for unfractured configurations and, for fractured configurations with one jump point, the curve provided by the system

$$\sigma = w'(u'), \quad w'(u') = \theta'([u]), \quad u' + l^{-1}[u] = \beta, \quad (11)$$

after elimination of $[u]$ and u' . The shape of the response curves is shown in Fig. 2b. The branch OH corresponds to unfractured configurations, while the fractured configurations may take different shapes depending on the geometric factor l , the length of the bar. The figure shows two possible shapes, one for large (L) and one for small (S) values of l . With respect to Griffith's model, the Barenblatt regularization brings two main improvements:

- (i) a *fracture threshold*: all metastable configurations with $\beta > \beta_H$ are fractured,
- (ii) the *size effect*: for $\beta > \beta_H$ the reduction of the force is gradual for small l , and sharp for large l .

Indeed, with reference to the figure, for large l one has $\sigma \simeq \sigma_H$ for β slightly less than β_H , and $\sigma < \sigma_K \ll \sigma_H$ for all $\beta > \beta_H$. The curves (S) and (L) reproduce the features of ductile fracture and of brittle fracture, respectively, and the difference in the two responses reflects the common observation that large bodies are more brittle than small bodies made of the same material.

3. A bi-modal energy [6] is characterized by the presence of two inflection points H,K which, as shown in Fig. 1, separate a central convex branch of the $(\theta, [u])$ curve from the two concave lateral branches. The metastability condition now allows for the presence of any number of jumps, provided that all jump amplitudes, except at most one, be in the range $([u]_H, [u]_K)$. The response of fractured configurations is now determined by the system

$$\sigma = w'(u'), \quad w'(u') = \theta'([u]_i), \quad u' + l^{-1} \sum_{j=1}^N [u]_j = \beta. \quad (12)$$

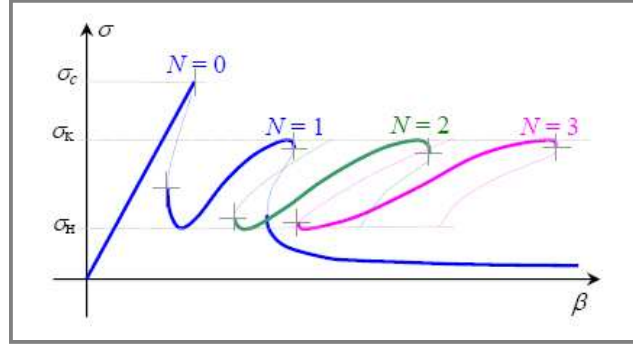


Figure 3: Response curves for a bi-modal cohesive energy, for large l .

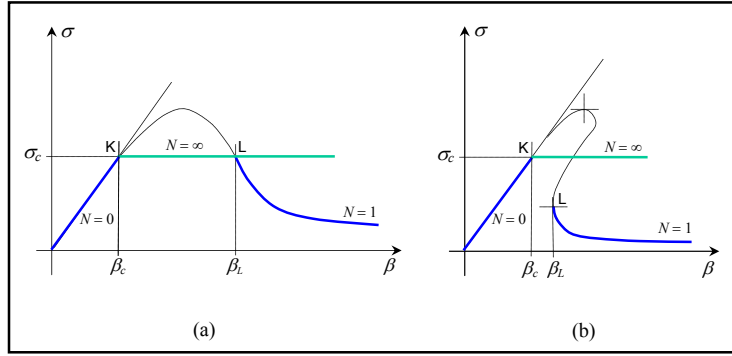


Figure 4: Response curves for a convex-concave cohesive energy for small (a) and for large (b) values of l .

It has a multiplicity of solutions, depending on the number N of the jumps. The shapes of the response curves are again influenced by the length l . The behavior for large l is shown in Fig. 3a: after reaching the fracture threshold at $\sigma = \sigma_c$, the axial force drops to σ_H . Then it grows to σ_K , it again drops at the opening of a second fracture, and so on. Thus, with growing β the force oscillates between σ_H and σ_K . As shown in the figure, at each new fracture opening the slope of the response curve decreases. This means that the level of damage in the bar increases with the number of fractures. In fact, with a proper choice of the expression of the cohesive energy it is possible to reproduce some experimental curves typical of damaged materials [5].

4. A convex-concave energy can be viewed as a bi-modal energy for which the inflection point H is sent to zero. According to the previous metastability analysis, the jumps must have an amplitude greater than $[u]_K$. Indeed, there is an interval larger than $(0, [u]_K)$ in which the equilibrium condition (7) is violated. Moreover, because $\theta''([u])$ is negative for all $[u] > [u]_K$, a metastable configuration has at most one jump.

The response curves for $N = 0$ and $N = 1$ are shown in Fig. 4, for small (a) and for large (b) values of l . From them one sees that, due to the initial convexity of θ , there is an interval (β_c, β_L) in which there are no metastable configurations. For these values of β it

seems reasonable to look whether an energy minimum can be attained at some *generalized solution*, obtained by suitably extending the domain of the energy functional. In fact, it is proved in [7] that the infimum for E is

$$\inf E = l(w(\beta_c) + \sigma_c(\beta - \beta_c)), \quad (13)$$

with σ_c and β_c defined by

$$\sigma_c \doteq w'(\beta_c) \doteq \theta'(0+), \quad (14)$$

and that the sequence $N \mapsto u_N$ in which $u'_N = \beta_c$ and each u_N has N jumps of equal amplitude

$$[u_N]_i = \frac{l}{N} (\beta - \beta_c) \quad (15)$$

is a minimizing sequence. The limit element of this sequence is then a global energy minimizer. But the limit element is of a special nature. One indeed can see that, for all x in $(0, l)$,

$$\lim_{N \rightarrow \infty} u_N(x) = \beta x, \quad \lim_{N \rightarrow \infty} u'_N(x) = \beta_c. \quad (16)$$

Therefore, $N \mapsto u_N$ converges uniformly to a continuous function. But the fact that the limit β_c of the derivatives does not coincide with the derivative β of the limit reveals that in the limit the jumps do not disappear, but diffuse across the beam becoming macroscopically invisible. In the language of measure theory, the distributional derivative of each u_N has a singular part represented by the jumps. In the limit, it transforms into the Cantor part of the derivative of the limit element. In the language of mechanics, this can be interpreted as the formation of a *microstructure*.

Because $\sigma = w'(u')$ and the u'_N are all equal to β_c , the response curve corresponding to the generalized solution is the horizontal line $\sigma = w'(\beta_c) = \sigma_c$ shown in Fig. 4. It is that this same curve may correspond to very different physical situations. Indeed, the energy minimization provides the number and amplitudes of the jumps, but not their location. Two examples made in [7] show the effect of uniform diffusion of the jumps and of their concentration on points of the Cantor set, respectively. An example in [4], Section 6.3, shows the effect of their concentration at a single point.

The above example show two main features of the cohesive energy model:

- (i) the model describes in a unified way a number of material responses, each corresponding to an appropriate choice of the analytic expression of the cohesive energy θ ,
- (ii) the response is determined by the shape of θ near the origin: initial concavity gives fracture-like behavior, and initial convexity gives plastic-like behavior.

3 Dissipative cohesive energy

The cohesive energy model leads to a satisfactory reproduction of the loading curves, but is inadequate to describe the response at unloading. Indeed, in the absence of any

source of dissipation, the response is totally reversible: fractures may heal, damage can be recovered, and plastic deformation can be eliminated at no energy cost.

For this reason, in [7] was introduced a second model which leaves unchanged the response at loading but, at the same time, provides a more realistic response at unloading. In the new model, the basic change is the assumption that the cohesive energy is totally dissipated. In this case one still has to minimize the total energy (1), now subject to a *dissipation inequality*

$$\theta'([u](x)) [\dot{u}](x) \geq 0, \quad (17)$$

which states that in an equilibrium process the cohesive energy cannot decrease at any point of the jump set. The minimization of elastic energy plus dissipation, formally proposed in [8], is now a standard tool to determine the quasi-static evolution of rate-independent materials [12].

In [7] is studied the case of θ' strictly positive, in which the dissipation inequality reduces to

$$[\dot{u}](x) \geq 0, \quad (18)$$

that is, to the requirement that the jump amplitudes can never decrease. This assumption leaves out some important cases, such as the case of *complete fracture*, see [7], Sect. 5.5. Here we make the same assumption, and we take (18) instead of (17) as the dissipation inequality.

A major effect of this supplementary restriction is that the equilibrium condition (6) now becomes an inequality:

$$\theta'([u](x)) \geq w'(u') \quad \forall x \in S(u). \quad (19)$$

Consequently, there are now many more equilibrium configurations. Indeed, the equilibrium configurations are not anymore only those represented by points on the response curves, but also all points located below the same curves. The following properties of the new equilibrium configurations are proved in [7]:

- (i) all equilibrium configurations u for which inequality (19) is strict at all jump points are metastable,
- (ii) for all such configurations the evolution is purely elastic. That is, $[\dot{u}](x) = 0$ for all equilibrium processes from u .

For configurations with at least one jump point at which inequality (19) is strict, the evolution of u is determined by an incremental minimum problem: given a *loading program* $t \mapsto \beta_t$ and an initial configuration u_0 equilibrated with β_0 , determine the increment \dot{u}_0 of u at $t = 0$.

This means to consider a formal expansion of u

$$u_t(x) = u_0(x) + t \dot{u}_0(x) + o(t), \quad (20)$$

and to minimize $E(u_t)$ for small t . It is proved in [7] that this problem reduces to the minimization of the quadratic functional

$$I([\dot{u}_0]_i) = w''(u'_0) \left(\frac{1}{l} \left(\sum_{S(u_0^{\parallel})} [\dot{u}_0]_i \right)^2 - 2\dot{\beta}_0 \sum_{S(u_0^{\parallel})} [\dot{u}_0]_i \right) + \sum_{S(u_0^{\parallel})} \theta''([u_0]_i) [\dot{u}_0]_i^2, \quad (21)$$

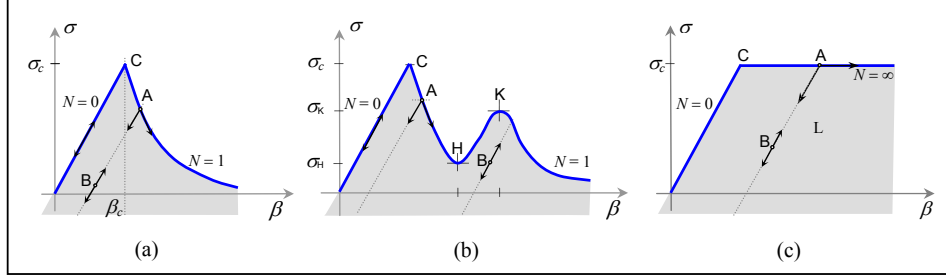


Figure 5: Directions of the quasi-static evolution in the dissipative model, for Barenblatt's (a), bi-modal (b), and convex-concave (c) cohesive energy. All curves refer to small values of l .

under the restrictions $[\dot{u}_0]_i \geq 0$. Here $S(u_0^\parallel)$ is the set of all jump points of u_0 at which (19) holds as an equality. It is also proved there that if all $\theta''([u_0]_i)$ have the same sign then the minimum is achieved at

$$[\dot{u}_0]_i = \frac{1}{\frac{l}{w''(u_0)} + \sum_{S(u_0^\parallel)} \frac{1}{\theta''([u_0]_j)}} l \dot{\beta}_0. \quad (22)$$

If M of them are negative and $N - M$ positive, then $[\dot{u}_0]_i = 0$ for all i for which $\theta''([u_0]_i) > 0$, and the remaining $[\dot{u}_0]_i$ are given by the above equation, with the sum restricted to the i with negative $\theta''([u_0]_i)$.

In Fig. 5 the gray areas represent the new equilibrium configurations introduced by the dissipative model. The arrows show the directions of the evolution, provided by the incremental minimization, at points A of the loading curve and B at the interior of the new equilibrium zones. These directions are parallel to the loading curve if the point is on the loading curve and $\dot{\beta}$ is positive, and parallel to the curve $N = 0$ in all other cases.

4 Future developments

To summarize, the cohesive energy model provides a unified approach to the analysis of material response, and the assumption of the dissipative character of the cohesive energy captures the differences between the responses at loading and at unloading. Nevertheless, many questions remain open. Namely,

- (i) both assumptions of a totally elastic and of a totally dissipative cohesive energy are extreme. Quite likely, a good choice could be to assume that the cohesive energy has a recoverable and a dissipative part,
- (ii) in a three-dimensional context, the bulk energy is diffused across the volume and the cohesive energy is concentrated on surfaces. Perhaps it would be more realistic to

assume that both are volume densities, and to obtain the localization of the cohesive energy on singular surfaces as a result of the minimization,

- (iii) an extension to higher dimension of the simple one-dimensional schemes examined here is far from trivial. It involves mathematical difficulties, for example, in the description of the singular sets at which the cohesive energy concentrates. There are also some uncertainties about the correct mechanical characterization.

References

- [1] Barenblatt, G.I., *The mathematical theory of equilibrium cracks in brittle fracture*, Adv. Appl. Mech. **7** (1962), 55-129.
- [2] Bourdin, B., Francfort, G., Marigo, J-J., *The variational approach to fracture*, J. Elasticity **91** (2008), 5-148.
- [3] Dal Maso, G., De Simone, A., Mora, M.G., *Quasistatic evolution problems for linearly elastic-perfectly plastic materials*, Arch. Ration. Mech. Anal. **180** (2006), 237-291.
- [4] Del Piero, G., *Foundations of the theory of structured deformations*, Multiscale Modeling in Continuum Mechanics and Structured Deformations, CISM Courses and Lectures N. **447** (Eds. G. Del Piero and D.R. Owen), Wien, Springer, 125-175, 2004.
- [5] Del Piero, G., *Bi-modal cohesive energies*, Variational Problems in Materials Sciences. Progress in Nonlinear Differential Equations and Their Applications, Vol. **68** (Eds. G. Dal Maso et al), Basel, Birkhäuser, 43-54, 2006.
- [6] Del Piero, G., Truskinovsky, L., *Macro- and micro-cracking in one-dimensional elasticity*, Int. J. Solids Structs. **38** (2001), 1135-1148.
- [7] Del Piero, G., Truskinovsky, L., *Elastic bars with cohesive energy*, Cont. Mech. Thermodyn., forthcoming.
- [8] Fedelich, B., Ehrlacher, A., *Sur un principe de minimum concernant des matériaux à comportement indépendant du temps physique*, C.R. Acad. Sci. Paris **308** (1989), 1391-1394.
- [9] Francfort, G.A., Garroni, A., *A variational view of partial brittle damage evolution*, Arch. Ration. Mech. Anal. **182** (2006), 125-152.
- [10] Francfort, G.A., Marigo, J-J., *Revisiting brittle fracture as an energy minimization problem*, J. Mech. Phys. Solids **46** (1998), 1319-1342.
- [11] Griffith, A.A., *The phenomenon of rupture and flow in solids*, Phil. Trans. Roy. Soc. London **A221** (1920), 163-198.
- [12] Mielke, A., *Evolution in rate-independent systems*, Handbook of Differential Equations, Vol. 2: Evolutionary equations (Eds. Dafermos C.M., Feireisl E.), Amsterdam, Elsevier, 461-559, 2005.

